

Secondary Organic Aerosol Formation from Isoprene Photooxidation

JESSE H. KROLL, NGA L. NG,
SHANE M. MURPHY,
RICHARD C. FLAGAN, AND
JOHN H. SEINFELD*

*Departments of Environmental Science and Engineering and
Chemical Engineering, California Institute of Technology,
Pasadena, California 91125*

Recent work has shown that the atmospheric oxidation of isoprene (2-methyl-1,3-butadiene, C₅H₈) leads to the formation of secondary organic aerosol (SOA). In this study, the mechanism of SOA formation by isoprene photooxidation is comprehensively investigated, by measurements of SOA yields over a range of experimental conditions, namely isoprene and NO_x concentrations. Hydrogen peroxide is used as the radical precursor, substantially constraining the observed gas-phase chemistry; all oxidation is dominated by the OH radical, and organic peroxy radicals (RO₂) react only with HO₂ (formed in the OH + H₂O₂ reaction) or NO concentrations, including NO_x-free conditions. At high NO_x, yields are found to decrease substantially with increasing [NO_x], indicating the importance of RO₂ chemistry in SOA formation. Under low-NO_x conditions, SOA mass is observed to decay rapidly, a result of chemical reactions of semivolatile SOA components, most likely organic hydroperoxides.

Introduction

As a substantial fraction of tropospheric particulate matter (PM) is composed of organic material, a detailed understanding of the sources and sinks of condensed organic compounds in the atmosphere is necessary to understand the effects of PM on the earth's climate and human health. A major source of uncertainty is the formation of secondary organic aerosol (SOA), particulate matter that is not emitted into the troposphere directly but rather is formed by gas-to-particle conversion of the oxidation products of volatile organic compounds (VOC's). At present, the global formation of SOA is poorly constrained, with estimates from modeling studies ranging from 12 to 70 Tg/year (1). Such estimates rely critically on laboratory measurements of the amount of SOA produced by individual SOA precursors, typically carried out in large environmental (smog) chambers. From these yield measurements, coupled with atmospheric models, it is now understood that the dominant contributors to global SOA are biogenic hydrocarbons (terpenes and sesquiterpenes), which form SOA primarily by reaction with the hydroxyl radical (OH) and ozone (O₃) (2). Anthropogenic hydrocarbons (most notably aromatic compounds) are also

believed to make a minor contribution to SOA on a global scale (3).

The global emission of biogenic terpenes and anthropogenic hydrocarbons is far lower than that of isoprene (2-methyl-1,3-butadiene, C₅H₈), estimated at ~500 Tg/year (4). Despite this large flux, isoprene has generally not been considered to be an SOA precursor, owing to the high volatility of its known reaction products. First-generation reaction products of the OH-isoprene reaction (under high-NO_x conditions) are well-characterized, with a measured carbon balance approaching 100%; structures and yields are shown in Figure 1. These products are too volatile to partition appreciably into the aerosol phase, and on this basis, isoprene is not expected to form SOA. Pandis et al. (12) and Edney et al. (13), for example, observed no aerosol growth from the photooxidation of isoprene under high-NO_x conditions.

Recent work suggests that isoprene may contribute to organic aerosol formation via heterogeneous reactions. Claeys and co-workers (14–16) have recently measured tetrols with the same carbon backbone as isoprene (as well as related compounds) in a number of atmospheric samples. Such species are likely to be formed by heterogeneous reactions; formation of tetrols has been observed in the aqueous-phase oxidation of isoprene in the presence of acid and hydrogen peroxide (17), as well as in the gas-phase photooxidation of isoprene in the presence of NO_x, SO₂, and ammonium sulfate seed (13). In the latter study only ~6% of the SOA mass observed could be identified (as tetrols and related products), suggesting the formation of other low-volatility compounds. In fact, Limbeck et al. showed (18) that polymeric, humic-like substances are formed when isoprene is passed through filters impregnated with sulfuric acid. Czoschke et al. (19) reported that the (very small) SOA yields from the ozonolysis of isoprene were enhanced in the presence of acidic seed particles, suggesting the polymerization of gas-phase oxidation reaction products as well. Matsunaga et al. (20, 21) measured high concentrations of second-generation isoprene oxidation products (hydroxyacetone, methylglyoxal, and glycolaldehyde) in aerosol samples, which may also suggest heterogeneous reactions leading to enhanced uptake. Additionally, modeling studies (22, 23) predict that water-soluble isoprene oxidation products will be scavenged by clouds, where they may be oxidized to lower-volatility compounds that remain in the condensed phase after droplet evaporation. Thus, isoprene may contribute to SOA via a number of heterogeneous chemical reactions, involving either polymerization or oxidation of isoprene and its reaction products.

In a recent study (24), we provided laboratory evidence that the gas-phase oxidation of isoprene indeed forms SOA. Isoprene oxidation was initiated by the photolysis of nitrous acid (HONO) in the presence of NO_x and ammonium sulfate seed, with SOA (yields of 0.9–3.0%) detected from isoprene concentrations as low as 60 ppb. At smaller concentrations, SOA yields could not be determined, due to the loss of particles to the walls, so SOA formation from isoprene oxidation under tropospheric conditions could not be determined. The difference in these results from those of Pandis et al. (12) and Edney et al. (13) likely arose from lower temperatures (20 °C vs 30 °C) and differences in oxidative conditions. SOA was shown to be formed from the oxidation of first-generation reaction products, but details of the underlying chemistry remain unclear. Many factors that may play a role in SOA formation have yet to be examined, such as reactions by different oxidants (OH, O₃, and NO₃), heterogeneous reactions (such as those outlined above), and NO_x concentration.

* Corresponding author phone: (626) 395-4635; fax: (626) 796-2591; e-mail: seinfeld@caltech.edu.

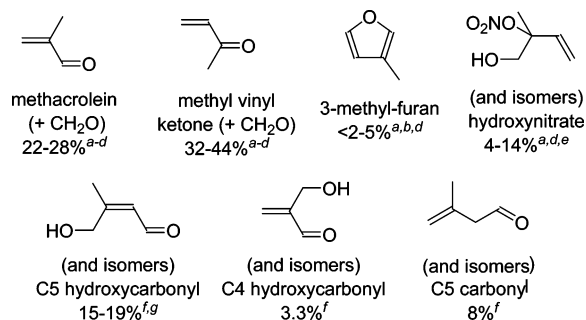


FIGURE 1. Structures and measured yields of first-generation products of the OH-initiated oxidation of isoprene under high-NO_x conditions. ^aTuazon and Atkinson (5). ^bPaulson et al. (6). ^cMiyoshi et al. (7). ^dSprengnether et al. (8). ^eChen et al. (9). ^fZhao et al. (10). ^gBaker et al. (11).

In the present study we examine SOA formation from isoprene in greater detail, to better understand the chemical mechanism of particle growth. The focus of this study is total SOA growth under varying reaction conditions (in particular NO_x and isoprene concentrations); the chemical composition of the SOA is beyond the scope of this work, and will be discussed in detail in a forthcoming paper. In these experiments, hydrogen peroxide (H₂O₂) is used as the radical precursor. H₂O₂ photolysis continually produces OH and HO₂ (from the OH + H₂O₂ reaction) over the course of the experiments, greatly simplifying the gas-phase chemistry. Gas-phase oxidation is dominated by reaction with OH (the primary oxidant of isoprene in the troposphere), with minimal interference by O₃ or NO₃. NO_x can be systematically varied over a wide range of concentrations by the addition of NO, and peroxy radical (RO₂) chemistry is relatively straightforward because any RO₂ formed will react only with HO₂ or NO. Additionally, here we use much lower seed particle loadings than in previous experiments, allowing for the precise measurement of small SOA volumes. From these measurements we are able to better constrain the chemical mechanism of SOA formation from isoprene oxidation, particularly the role of peroxy radicals.

Experimental Section

Experiments are carried out in Caltech's dual 28 m³ FEP Teflon chambers, described in detail elsewhere (25, 26). The chambers are surrounded by banks of blacklights (276 GE350BL) and aluminum sheets for maximum reflectivity. Numerous ports allow both for the introduction of clean air, gas-phase reagents, and inorganic seed, and for various gas-phase and particulate measurements. A differential mobility analyzer (DMA, TSI 3760) measures the size distribution and volume concentration of particles inside the chambers; settings are the same as described in Keywood et al. (26). In most experiments, an Aerodyne Time-of-Flight aerosol mass spectrometer (AMS, described in detail in ref. 27) is also used, for the measurement of mass distributions of particulate organics, sulfate, nitrate, and ammonium. A gas chromatograph coupled with flame ionization detection (GC-FID, HP 5890) allows for the measurement of gas-phase isoprene. GC-FID response is calibrated by sampling from a 60 L FEP Teflon bag into which known volumes of isoprene have been introduced. Temperature, relative humidity (RH), O₃, NO, and NO_x are all continually monitored. Experiments are run in each chamber on alternating days; the chamber that is not in use on a given day is repeatedly flushed with clean air and irradiated with UV light for cleaning.

The radical precursor used in the present experiments is hydrogen peroxide. H₂O₂ is introduced by bubbling 5 L/min of humidified room-temperature air for 2 1/2 hours through

a 50% H₂O₂ solution (Aldrich), through a particle filter to avoid the introduction of droplets, and finally into the chamber. The concentration of H₂O₂ is not measured directly, but from the rate of isoprene decay during irradiation, and literature values of $\sigma_{\text{H}_2\text{O}_2}$, $k_{\text{OH}+\text{isoprene}}$, and $k_{\text{OH}+\text{H}_2\text{O}_2}$ (28, 29), [H₂O₂] is estimated to be ~3–5 ppm; this may decrease somewhat over the course of the experiment due to wall loss, photolysis, and reaction with OH. To minimize potential uptake of H₂O₂ into the particle phase, all experiments are run under dry (RH < 10%) conditions. These conditions are substantially drier than those of the troposphere. The dependence of SOA growth on RH is beyond the scope of this work but warrants future investigation.

After introduction of H₂O₂, ammonium sulfate seed (if used) is introduced by atomization of a 0.015 M solution of (NH₄)₂SO₄ at 30 psi; initial volume concentrations are 4.6–7.1 μm³/cm³. For high-NO_x experiments, a known quantity of NO is then introduced from a 500 ppm gas cylinder (in N₂, Scott Specialty Gases). Typically, some fraction (20–40 ppb) is immediately converted to NO₂, likely from reactions with residual O₃ and NO₃/N₂O₅ in the chamber, and so the chamber is free of any oxidants when hydrocarbon is added. Isoprene (12–90 ppb) is introduced by sending air over a measured volume of the pure compound (Aldrich, 99.8%) and into the chamber.

When all components are well-mixed (measured values of isoprene, NO_x, and seed particle volume are constant), the blacklights are turned on, initiating photooxidation and the beginning of the experiment. Output from the lights in the ultraviolet is between 300 and 400 nm, with a maximum at 354 nm. The very weak absorption cross section of H₂O₂ in this range necessitates the use of more lights than in our prior study using HONO (24); half the available lights are used in the present experiments. Using measurements of photon flux inside the chamber enclosure and known absorption cross sections (28), we calculate J_{NO_2} and $J_{\text{H}_2\text{O}_2}$ to be 0.29 min⁻¹ and 0.00029 min⁻¹, respectively; hence, ppm concentrations of H₂O₂ are required. Heating from the lights leads to a temperature increase inside the chamber of approximately 5 °C over the course of the experiment. The DMA and AMS are both located outside the chamber enclosure and are at the temperature of the surrounding room (~20–22 °C). Thus, the air may cool slightly as it is sampled from the chamber and into the instruments, and the measured aerosol is likely to correspond to gas-particle partitioning at the temperature of the room rather than the temperature at which the gas-phase chemistry occurs. Such temperature differences (≤5 °C) are unlikely to affect results significantly.

Results

Blank Runs. To ensure that all SOA growth observed is indeed from isoprene photooxidation, blank runs are performed regularly over the course of the data collection. Minimal growth (<0.1 μg/m³) is observed from irradiation of mixtures of H₂O₂, NO_x, and/or inorganic seed (with no isoprene present). In addition, from the measured SOA yields and mass spectra, the particle growth observed cannot be the result of a small terpene impurity (~0.2%) in the isoprene. These results are described in detail in the Supporting Information.

Low-NO_x Experiments. Shown in Figure 2 is a typical low-NO_x experiment ([NO_x] < 1 ppb), in which 63.6 ppb isoprene is oxidized in the absence of inorganic seed. Particles are detected after ~40 min of irradiation; aerosol growth is measured using both the DMA and AMS and occurs mostly after all the isoprene has been reacted. AMS data confirm that the new particle mass is organic, with a typical mass spectrum shown in Figure 3. Ozone formation (not shown in Figure 2) of a few ppb is observed, possibly due to residual

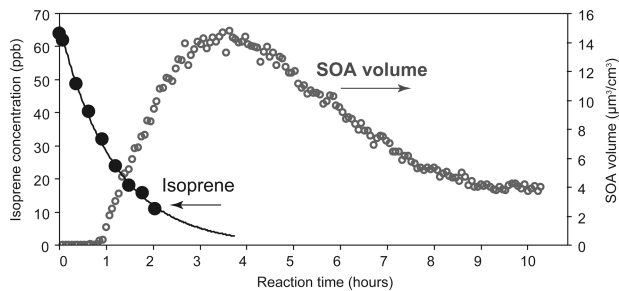


FIGURE 2. Reaction profile of a typical isoprene photooxidation experiment under NO_x -free conditions (Experiment 5).

NO_x emitted by the chamber walls. Such small O_3 concentrations are unlikely to have any appreciable effect on the gas-phase chemistry. After an initial period of aerosol growth, aerosol mass and volume are observed to decrease rapidly to lower final values. This is not a result of the loss of particles to the walls, as it is characterized by a shrinking of the aerosol size distribution rather than a decrease in number concentration. The loss of aerosol mass stops immediately when the lights are turned off, and resumes when the lights are turned back on, suggesting it is not caused by gradual changes in temperature or RH. Possible mechanisms are examined in the Discussion section.

Aerosol growth from isoprene photooxidation is also observed at lower isoprene concentrations (and, hence, smaller organic aerosol loadings). The DMA detects SOA from isoprene concentrations as low as 12.2 ppb; below that, the signal-to-noise is too poor for the detection of growth. Aerosol growth is detected at still lower isoprene concentrations (~ 8 ppb) by the AMS. The mass spectra of the SOA, at maximum growth and at the end of the experiment, are similar to those from the higher-concentration experiments, indicating that SOA formation is indeed significant, even at such low isoprene concentrations and particulate loadings.

Experimental conditions and results from all low- NO_x experiments are given in Table 1. For all these experiments, no inorganic seed is added; the small size of nucleated particles leads to good signal-to-noise of the DMA volume measurement so that very small growths ($< 1 \mu\text{m}^3/\text{cm}^3$) can be measured. Measured increases in aerosol volume are found to be largely insensitive to the presence of ammonium sulfate seed. Two values for the increase in aerosol volume are given in Table 1: "maximum growth" (before the rapid loss of SOA dominates) and "final growth" (once SOA volume and mass have leveled out). All volumes are corrected for losses to the chamber walls, by applying size-dependent first-order loss coefficients, estimated by running "seed-only" experiments in the absence of hydrocarbon (26). SOA yield,

TABLE 1. Experimental Conditions and Results for NO_x -free Experiments^a

expt. no.	isoprene reacted (ppb)	ΔM_0 (max) ($\mu\text{g}/\text{m}^3$) ^b	ΔM_0 (final) ($\mu\text{g}/\text{m}^3$) ^b	SOA yield (%) ^c	T_{max} ($^\circ\text{C}$)
1	90.0	27.0 ± 0.5	9.3 ± 0.4	3.6 ± 0.1	25.4
2	46.1	13.5 ± 0.6	3.8 ± 0.5	2.9 ± 0.3	25.6
3	23.0	2.3 ± 0.5	0.6 ± 0.3	0.9 ± 0.4	26.0
4	12.2	0.7 ± 0.1	0.3 ± 0.1	1.0 ± 0.3	25.7
5	63.6	17.8 ± 0.5	5.0 ± 0.5	2.8 ± 0.3	26.7
6	29.4	6.2 ± 0.8	2.2 ± 0.5	2.6 ± 0.6	28.7
7	47.8	11.1 ± 0.5	3.0 ± 0.4	2.2 ± 0.3	26.6
8	41.6	8.4 ± 0.4	2.4 ± 0.5	2.1 ± 0.5	26.4

^a Stated uncertainties (2σ) are from scatter in particle volume measurements. ^b Assuming an SOA density of $1.25 \text{ g}/\text{cm}^3$. ^c SOA yields from final growth only.

defined as the ratio of mass concentration of SOA formed to mass concentration of isoprene reacted, is given for the final growth only. This requires knowledge of the SOA density, determined by a comparison of aerosol volume (from the DMA) and aerosol mass (from the AMS), as described by Bahreini et al. (30). Density is determined to be $1.25 (\pm 0.1) \text{ g}/\text{cm}^3$ for SOA formed under low NO_x conditions. As is typical for SOA-forming reactions, yields are found to vary with the amount of hydrocarbon reacted (31, 32); the dependence of aerosol growth (both maximum and final growth) on the amount of isoprene reacted is illustrated in Figure 4.

High- NO_x Experiments. The addition of NO to the reaction mixture has a large effect on the gas-phase chemistry, as illustrated in Figure 5 for a typical experiment (42.7 ppb isoprene, 98 ppb NO, 31 ppb NO_2 , $6.4 \mu\text{m}^3/\text{m}^3$ seed). Isoprene decay is far faster than in the low- NO_x case, due to regeneration of OH from the $\text{HO}_2 + \text{NO}$ reaction. This reaction also rapidly converts NO to NO_2 . Ozone formation, from NO_2 photolysis, begins once $[\text{NO}]$ falls below ~ 50 ppb. When $[\text{NO}]$ approaches zero (concentrations of a few ppb), aerosol growth is observed. Aerosol mass and volume typically reach a maximum after ~ 4 h into the reaction; unlike in the low- NO_x case, no rapid loss of SOA is observed.

The mass spectrum of SOA formed from isoprene under typical high- NO_x conditions is shown in Figure 6. SOA composition is clearly different from that formed under NO_x -free conditions (Figure 3), with mass fragments displaying a more ordered, repetitive pattern. Aerosol growth is also observed from the oxidation of ~ 8 ppb isoprene (with 280 ppb NO); the mass spectrum is again the same as that from higher concentrations of isoprene (see Supporting Information).

Measurements of aerosol growth and SOA yield over a range of isoprene concentrations were not carried out for

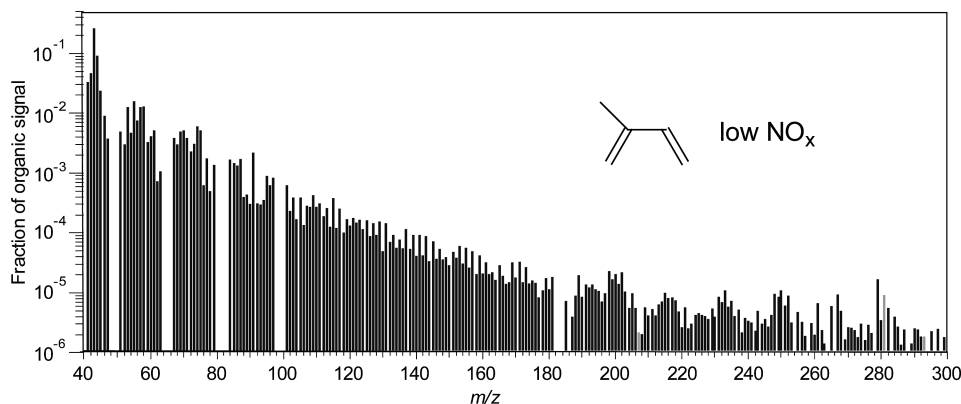


FIGURE 3. Typical AMS spectrum ($m/z \geq 40$) of SOA formed from isoprene photooxidation under low- NO_x conditions. For clarity, masses in which the organics overlap with peaks from sulfate (m/z 48–50, 64–66, 80–83, 98–100) and tungsten (from the filament; m/z 182, 184–186) have been omitted. Light gray bars correspond to negative values after data analysis.

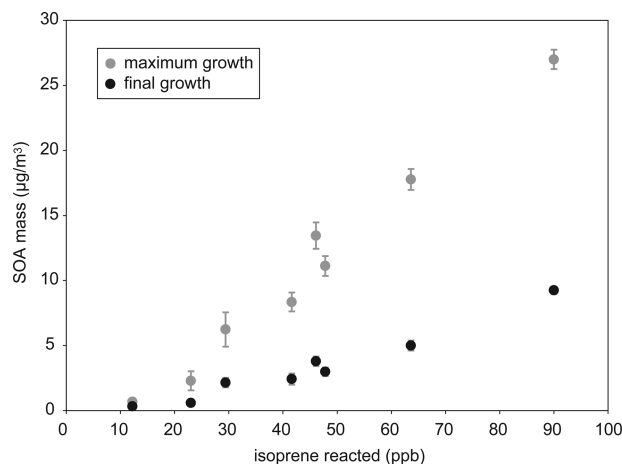


FIGURE 4. Measured SOA growth versus isoprene reacted (low- NO_x conditions). Gray circles: maximum growth; black circles: final growth, after photochemical loss of SOA (see text for details). Each pair of points (at a single value of isoprene reacted) corresponds to one experiment. Data are taken from Table 1; SOA mass is calculated using a density of 1.25 g/cm^3 .

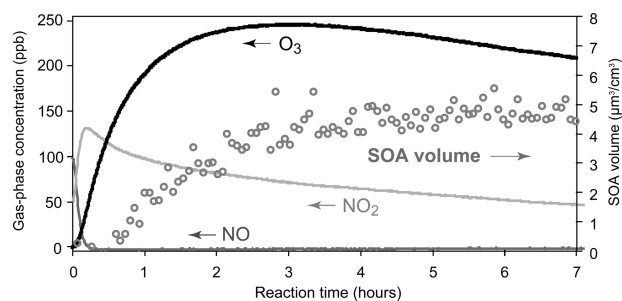


FIGURE 5. Reaction profile of a typical isoprene photooxidation experiment under high- NO_x conditions (Experiment 11). Decay of isoprene is rapid, with most consumed in the first 30 min of reaction, so it is omitted for clarity.

the high- NO_x case because we have presented such results previously (24). Instead, we focus on the dependence of SOA growth on NO_x concentration, in which initial isoprene concentrations are held essentially constant ($45 \pm 4 \text{ ppb}$). Shown in Table 2 are experimental conditions and results for the high- NO_x experiments. Ammonium sulfate seed is used in all cases to provide surface area onto which semivolatile products may condense. Running the reaction in the absence of seed leads to the formation of large number concentrations ($50\,000\text{--}150\,000 \text{ particles/cm}^3$) of very small particles, due to the fast rate of formation of condensable products. Such small particles are lost to the walls very quickly, precluding accurate (wall-loss-corrected) volume measurements, so seed particles are necessary. Under high- NO_x conditions, SOA density is determined to be $1.35 (\pm 0.05) \text{ g/cm}^3$. Shown in Figure 7 is SOA growth versus initial NO_x concentration. The SOA yields measured in these experiments are somewhat higher than those reported in our previous study (24); this may be a result of differences in gas-phase chemistry (such as initial $[\text{NO}_x]$, rate of change of $[\text{NO}_x]$, and the $[\text{NO}]:[\text{NO}_2]$ ratio), photolytic conditions, and/or RH. Understanding these possible effects requires further study. We note that in one previous photooxidation study (33), no RH-dependence of SOA yields was observed.

Isoprene Oxidation Products. Two additional studies are carried out in which methacrolein (500 ppb, Aldrich, 95%) and methyl vinyl ketone (500 ppb, Aldrich, 99%) are photooxidized under high- NO_x conditions (initial $[\text{NO}_x] = 860 \text{ ppb}$). While the oxidation of methyl vinyl ketone produces no SOA,

methacrolein oxidation produces substantial SOA ($170 \pm 1 \mu\text{m}^3/\text{cm}^3$), as reported previously in an experiment using HONO as the radical precursor (24). The AMS spectrum of SOA from methacrolein oxidation is shown in Figure 8.

Discussion

General Mechanism of SOA Growth. In both the low- and high- NO_x experiments, SOA growth does not begin until a significant fraction ($>50\%$) of the isoprene is consumed, and SOA growth continues even after the isoprene is fully consumed. This implies the existence of a rate-limiting step in SOA formation following the initial OH-isoprene reaction. As discussed in previous work (24), this step is likely the oxidation of first-generation reaction products; both double bonds of isoprene must be oxidized, resulting in the addition of up to four polar functional groups to the carbon skeleton. This conclusion is strongly supported by the observation of SOA production from the oxidation of methacrolein, a major first-generation isoprene oxidation product. The role of second-generation products in SOA formation (from the oxidation of isoprene and other biogenic hydrocarbons) is discussed in detail by Ng et al. (34).

Shown in Figure 9 is the simplified mechanism of the initial steps of the OH + isoprene reaction, leading to the formation of first-generation molecular products. The hydroxyl radical adds to one of the double bonds, primarily at the 1- or 4-position, and the subsequent addition of O_2 leads to the formation of six possible isoprene hydroxperoxy radicals (for simplicity, only one is shown in Figure 9). The fate of this radical depends on the level of ambient NO_x . At high NO_x ($[\text{NO}] \gg [\text{HO}_2] + [\text{RO}_2]$), peroxy radicals primarily react with NO. They may also react with NO_2 to form peroxy nitrates (RO_2NO_2), but these are thermally unstable, with lifetimes shorter than 1s, so they are generally unimportant under most conditions. Isoprene hydroxperoxy radicals plus NO forms either hydroxynitrates or hydroxy-alkoxy radicals, the latter of which undergo decomposition, isomerization, or hydrogen abstraction by O_2 to form methacrolein, methyl vinyl ketone, and other first-generation isoprene oxidation products shown in Figure 1.

The rates and products of the oxidation reactions of many of these first-generation products are poorly constrained. The oxidation reactions of methacrolein and methyl vinyl ketone are well-studied, with known products accounting for $>90\%$ of the total reaction (35–37). Based on our observation of SOA production from methacrolein oxidation, it is clear that some products of the OH-methacrolein reaction (possibly minor, previously undetected species) are condensable. The similarity between the mass spectrum of SOA from methacrolein oxidation (Figure 8) and that of isoprene oxidation (Figure 6) strongly suggests that methacrolein is a principal intermediate in SOA formation from isoprene photooxidation under high- NO_x conditions. It is not straightforward to quantify the contribution of methacrolein oxidation products to SOA from isoprene oxidation, due to the dependence of gas-particle partitioning on available organic particulate matter (31, 34). Products of the oxidation of other first-generation products, accounting for 20–40% of the OH + isoprene reaction, have, for the most part, not been measured, but may also play a role in SOA formation.

The oxidation of isoprene under low- NO_x conditions has received far less study and so is more uncertain. When concentrations of peroxy radicals (HO_2 and RO_2) approach the concentration of NO, $\text{RO}_2 + \text{HO}_2$ and $\text{RO}_2 + \text{RO}_2$ reactions become competitive with $\text{RO}_2 + \text{NO}$, and a different product distribution is expected (lower half of Figure 9). The reaction of isoprene hydroxperoxy radicals with other RO_2 radicals is expected to lead to a mixture of hydroxycarbonyls, diols, and products from alkoxy radical reactions, such as methacrolein and methyl vinyl ketone, all of which have been

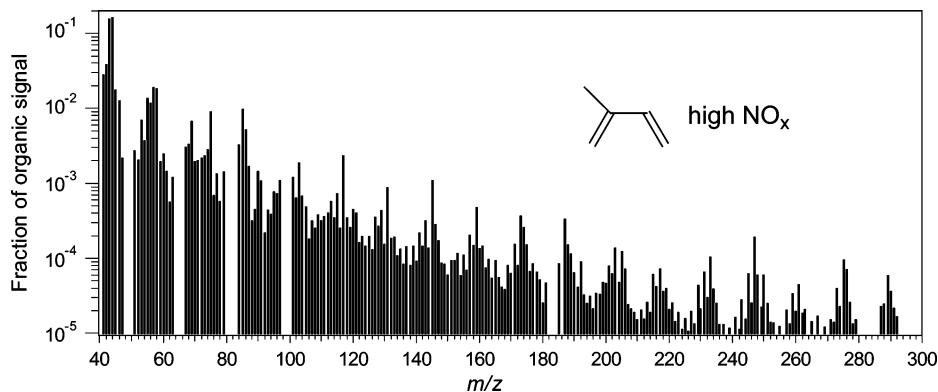


FIGURE 6. Typical AMS spectrum of SOA formed from isoprene photooxidation under high- NO_x conditions. See description of Figure 3 for details.

TABLE 2. Experimental Conditions and Results for High- NO_x Experiments^a

expt. no.	isoprene reacted (ppb)	initial [NO] (ppb)	Initial [NO _x] (ppb)	(NH ₄) ₂ SO ₄ volume (μm ³ /cm ³)	maximum [O ₃] (ppb)	ΔM ₀ (μg/m ³) ^b	SOA yield (%)	T _{max} (°C)
9	46.7	242	266	4.6 ± 0.2	342	6.3 ± 1.0	4.7 ± 0.7	28.3
10	43.5	496	526	7.1 ± 0.3	389	2.9 ± 1.2	2.3 ± 0.9	28.3
11	42.7	98	129	6.4 ± 0.7	245	6.7 ± 1.3	5.5 ± 1.0	28.1
12	49.1	51	78	6.5 ± 0.3	256	5.6 ± 1.3	4.0 ± 0.9	28.2
13	42.7	337	405	4.8 ± 0.2	508	4.6 ± 1.0	3.8 ± 0.8	28.3
14	42.0	708	745	4.7 ± 0.3	492	1.7 ± 1.1	1.4 ± 0.9	27.5

^a Stated uncertainties (2σ) are from scatter in particle volume measurements. ^b Assuming an SOA density of 1.35 g/cm³.

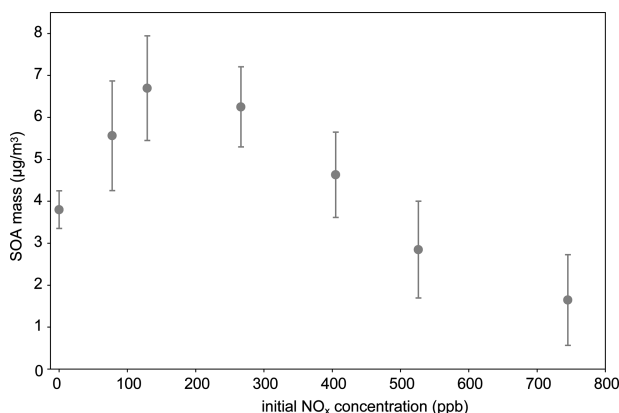


FIGURE 7. SOA growth as a function of initial NO_x concentration, for a fixed isoprene concentration (45 ± 4 ppb). Results shown are from Table 2; the NO_x -free point is final growth from Experiment 2, Table 1.

detected in the laboratory (7, 38–40); yields and carbon balance are not fully established. The hydroxyhydroperoxides expected from the reaction of HO_2 with isoprene RO_2 radicals have not been conclusively identified in the laboratory, though they have been tentatively identified in the troposphere (41). Miyoshi et al. (7) found that under conditions in which the $\text{HO}_2 + \text{RO}_2$ reaction dominates, organic hydroperoxides are formed in high concentrations with no other identifiable gas-phase products. The further reactions of these oxidation products have not been studied. In particular, the tropospheric fate of isoprene hydroxyhydroperoxides is highly uncertain, and the relative importance of photolysis and reaction with OH is largely unknown, as is the product distribution from each channel.

In summary, the lack of experimental data on the second-generation products (and, at low NO_x , even the first generation products) of isoprene oxidation makes it difficult to know the exact chemical mechanism of SOA formation. Under high- NO_x conditions, methacrolein is certainly an important

intermediate in the production of SOA. Numerous pathways may be put forth which lead to the formation of relatively nonvolatile second-generation oxidation products, with 4–5 carbon atoms and 3–4 polar functional (carbonyl, hydroxy, hydroperoxy, nitrate, or acid) groups. Further studies of the gas- and particle-phase products of isoprene oxidation would be useful for identifying the detailed chemistry of SOA formation.

In addition, particle-phase reactions of these products are likely to contribute to SOA formation. From the aerosol mass spectra (Figures 3, 6, and 8), it is clear that oligomers are formed. At both high- and low- NO_x , a significant fraction of the organic mass is from fragments of high molecular weight ($m/z > 200$), corresponding to species with more than five carbon atoms (C5 products will have masses ≤ 226 , the mass of the dihydroxy-dinitrate). An important role of such reactions in SOA formation may explain why methacrolein oxidation forms SOA but methyl vinyl ketone oxidation does not, as aldehydes are substantially more susceptible to nucleophilic attack (and hence oligomerization reactions) than are ketones (42). The chemical composition of the SOA will be discussed in detail in a forthcoming publication.

Role of NO_x . Despite uncertainties in the detailed chemical mechanism of isoprene oxidation, the dependence of SOA growth on NO_x level (Figure 7) provides some insight into the underlying chemistry of SOA formation. At high NO_x (>200 ppb), SOA yield is found to decrease with increasing NO_x ; similar decreases have been observed in a number of SOA yield measurements (12, 43–49). This dependence has been attributed to two effects: (1) relative levels of different oxidants (OH, NO_3 , and O_3) present in the reaction system (45), and (2) the chemistry of peroxy radicals (43, 46, 49). In the present study, OH is the dominant oxidant throughout the course of the experiment, due to the continual production of OH radicals from H_2O_2 photolysis. The O_3 and NO_3 produced in the high- NO_x experiments account for a negligible fraction of the isoprene reacted, because they are only formed once NO concentration is near zero, typically

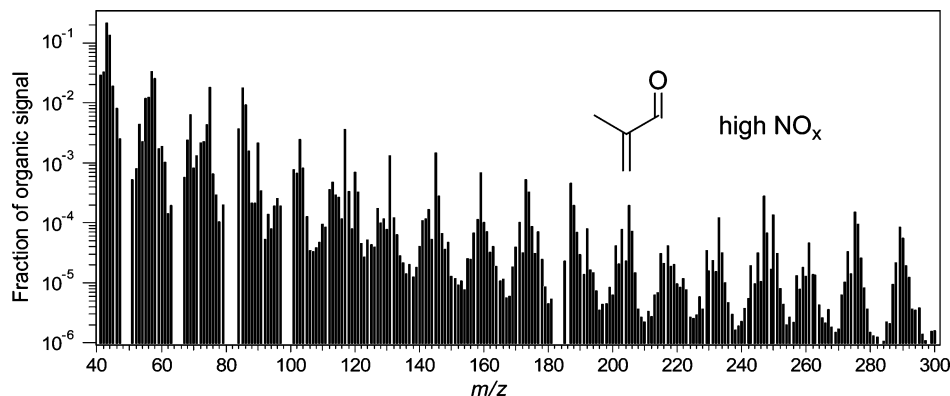


FIGURE 8. AMS spectrum of SOA formed from methacrolein photooxidation under high- NO_x conditions. See description of Figure 3 for details. The spectrum shown is similar to that of isoprene photooxidation (Figure 6), with the same major peaks, suggesting the importance of methacrolein as an intermediate in SOA formation from isoprene oxidation under high- NO_x conditions.

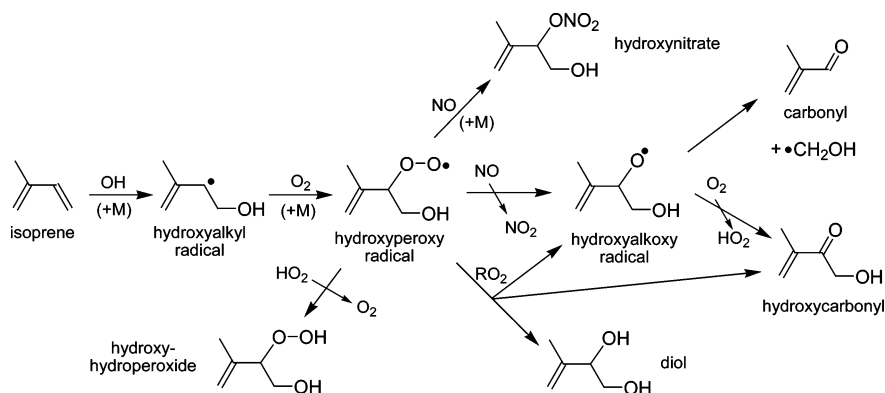


FIGURE 9. Reaction mechanism of isoprene oxidation, showing the formation of first-generation products. For clarity, only one of four possible alkyl radicals and one of six possible hydroperoxy radicals are shown. The first-generation reaction products are all unsaturated so they may be rapidly oxidized to second-generation products.

after all isoprene has been reacted away. Isoprene oxidation products may react with O_3 or NO_3 , but for major oxidation products, such reactions are slow (29) and are expected to be unimportant. There may, however, be exceptions (for example, 3-methyl-furan reacts rapidly with NO_3 (50)), and we cannot rule out the possibility that reactions of O_3 or NO_3 may be sinks for minor isoprene oxidation products.

Nonetheless, all of the oxidation of isoprene, and the oxidation of most of its reaction products, is initiated by the OH radical; the observed NO_x dependence of SOA yields is likely a result not of differences in OH, O_3 , and NO_3 reactions, but of rather differences in peroxy radical chemistry. In the present experiments, organic peroxy radicals will react with either HO_2 (formed in the OH + H_2O_2 reaction) or NO. RO_2 + RO_2 reactions are relatively unimportant because the concentration of H_2O_2 (which reacts with OH to form HO_2) is much higher than that of isoprene (which reacts with OH to form RO_2), and HO_2 + RO_2 reactions are significantly faster than RO_2 self-reactions (51). As mentioned above, peroxy-nitrate formed from RO_2 + NO_2 serves as only as a short-lived reservoir of RO_2 . Thus the fate of RO_2 radicals depends on the relative concentrations of HO_2 and NO. At high [NO], alkoxy radicals and organic nitrates will be formed from the RO_2 + NO reaction; small alkoxy radicals are expected to fragment, and organic nitrates may be relatively volatile (49). On the other hand, at low [NO], RO_2 + HO_2 reactions form hydroperoxides, recently shown in both experimental (52) and modeling (46, 53, 54) studies to be important components of SOA. High concentrations of NO, therefore, appear to suppress the formation of SOA by suppressing hydroperoxide formation, consistent with the conclusions of other studies of the NO_x -dependence of SOA formation (43, 46, 49). This also explains our observations that SOA growth begins only

when NO concentrations approach zero, which appears to be a general feature of chamber measurements of SOA formation from hydrocarbon photooxidation (e.g., 45–47, 54). As discussed previously (24), in the studies of Pandis et al. (12) and Edney et al. (13), [NO] did not fall below ~ 30 ppb, and no SOA was produced. Thus the formation of hydroxyhydroperoxides is likely to play an important role in SOA formation from isoprene photooxidation. This is consistent with the results of Miyoshi et al. (7), who report the formation of both gas-phase hydroperoxides and particles from the OH + isoprene reaction at low NO_x and high HO_2 . In the particle phase, hydroperoxides may react further, oxidizing organics or reacting with aldehydes to form peroxyhemiacetals (55), oligomeric species which may account for some of the high-MW peaks seen in AMS spectra of SOA (Figure 6).

However, the suppression of SOA formation by NO does not fully explain the observed NO_x -dependence of aerosol yields from isoprene photooxidation, as yields increase with NO_x at low NO concentrations (Figure 7). Similar NO_x -dependences of aerosol yield have been observed in the photooxidation of α - and β -pinene (12, 44); however, those experiments were carried out under very different oxidative conditions than in the present study and so may not be directly comparable. The increase in SOA growth with NO_x may be the result of changes in reaction conditions over the course of the experiments; over time the [NO]/[HO_2] ratio decreases (as NO is converted to NO_2 , and the suppression of HO_2 by NO decreases), which may lead to a switch from high- NO_x to low- NO_x conditions. This could lead to a complex dependence of SOA formation on NO_x ; peroxy radicals formed in the first oxidation step (OH + isoprene) react with NO, whereas peroxy radicals formed by the oxidation of isoprene

reaction products react with HO₂. Such a change in NO_x conditions may be relevant in the troposphere during transport from a polluted to an unpolluted region, but it would be preferable to measure SOA yields under conditions in which the [NO]/[HO₂] ratio, and thus the fate of organic peroxy radicals, stays constant over the course of the entire experiment. More generally, to apply chamber results to atmospheric conditions, it is important that the [NO]/[HO₂] ratio be well-constrained; in our experiments, SOA is suppressed by 100s of ppb of NO, though in the atmosphere this is likely to occur at lower NO concentrations due to elevated HO₂ concentrations (estimated at 100s of ppt) in the chamber. Thus, reaction conditions need to be better controlled and characterized before parameterizations of SOA yields as a function of [NO_x] may be obtained.

It should be noted that the NO_x-dependence of SOA growth measured in this work may not apply generally to all SOA-forming reactions. For example, Edney et al. (13) showed that, in the presence of SO₂, isoprene oxidation forms SOA even in the presence of NO, suggesting that enhanced reactive uptake by acidic aerosol particles may counteract the reduced production of condensable species at high NO_x. Additionally, the reaction of NO with large peroxy radicals will form alkoxy radicals which isomerize rather than fragment. These will form large, multifunctional products, which may efficiently partition into the aerosol phase. Thus hydrocarbons substantially larger than isoprene are expected to form SOA even under high-NO_x conditions. Indeed, recently SOA formation from the OH-initiated oxidation of long-chain alkanes has been observed in the presence of several ppm of NO (56). In such cases, SOA yields may even be higher at high NO_x. Thus SOA formation may be a complex function of NO_x level, and future study is required.

Rapid Photochemical Loss of SOA. As noted earlier, under low-NO_x conditions ([NO_x] < 1 ppb), initial SOA growth from isoprene oxidation is large (sometimes reaching yields of > 10%), but is followed by a rapid decrease in aerosol volume as the reaction progresses (Figure 2). To our knowledge such an effect has not been reported in previous chamber studies of SOA formation. The decrease in SOA, characterized by a shrinking of particles rather than a reduction in particle number, is a photochemical effect, as it occurs only during chamber irradiation (when UV photons and OH radicals are present), ceasing immediately when the chamber lights are turned off. Therefore, this may be an example of photochemical "aging", or oxidative processing, of the SOA. We do not observe rapid loss of SOA formed in the low-NO_x photooxidation of β-pinene (140 ppb), indicating that it is not a general feature of the irradiation of all hydrocarbon/H₂O₂ mixtures.

The photochemical mechanism of volatilization is not clear at present. Recent experimental evidence shows that the reaction of gas-phase OH radicals with condensed organics may lead to efficient volatilization of organic compounds, thereby serving as a sink for SOA in the troposphere (57). However, such a mechanism probably cannot account for the fast rate of SOA loss observed, and we observe no obvious dependence of the rate of SOA loss on surface area, which would be expected for reactions of gas-phase oxidants with condensed-phase organics.

Instead, the SOA loss may be a result of gas-phase or particle-phase oxidation reactions continuing after particle formation. Once semivolatile compounds reach gas-particle equilibrium, any further gas-phase losses (by reaction with OH or photolysis) of those compounds may drive equilibrium away from the particle phase, leading to a decrease in SOA mass. If all losses are from such gas-phase reactions, and these reactions (rather than gas-particle partitioning) are the rate-limiting step, then the SOA loss (0.006–0.018 min⁻¹) is consistent with the reaction with OH (*k*_{OH} = 4.0 × 10⁻¹¹–1.2

× 10⁻¹⁰ cm³ molec⁻¹ s⁻¹ for [OH] = 2.5 × 10⁶/cm³), photolysis (*J* = 0.006–0.018 min⁻¹), or some combination of the two. Given that this effect is seen only at low NO_x, these reactive compounds are likely to be organic hydroperoxides. If loss is by photolysis, the inferred *J* value is significantly larger (by 1 or 2 orders of magnitude) than that of the simplest organic peroxide, CH₃OOH (29). The efficient photolysis of organic hydroperoxides has been put forth as an explanation for discrepancies between measured tropospheric ozone production and modeled HO_x chemistry (58), as well as for the observation that SOA yields from α-pinene ozonolysis are lower under UV irradiation than under dark conditions (59). In the latter case, the underlying chemistry (and inferred photolytic lifetime) is substantially different than in the present study, but it is clear that the photochemistry of structurally complex organic peroxides deserves further study.

However, gas-phase reaction is unlikely to account for all of the observed loss, as AMS results show that the chemical composition of the SOA changes over the course of the decrease; a number of high-MW organic fragments are observed to increase in intensity even during the rapid loss of organic aerosol mass. This may be a result of particle-phase reactions, such as the photolysis of condensed-phase hydroperoxides. Such reactions would form OH and alkoxy radicals within the aerosol, which would serve to rapidly oxidize other SOA components; products of such reactions may be quite volatile, leading to the loss of SOA mass, or oligomeric and highly nonvolatile. In a forthcoming publication, in which we focus on the chemical composition of SOA from isoprene oxidation, the chemistry of this photochemical aging process will be explored in greater detail.

Acknowledgments

This research was funded by the U.S. Environmental Protection Agency Science to Achieve Results (STAR) Program grant number RD-83107501-0, managed by EPA's Office of Research and Development (ORD), National Center for Environmental Research (NCER), and by the U.S. Department of Energy Biological and Environmental Research Program DE-FG03-01ER63099; this work has not been subjected to the EPA's required peer and policy review and, therefore, does not necessarily reflect the views of the Agency and no official endorsement should be inferred.

Supporting Information Available

Details of the blank runs, tests for the role of impurities, and low-concentration runs. This material is available free of charge via the Internet at <http://pubs.acs.org>.

Literature Cited

- 1) Kanakidou, M.; et al. Organic aerosol and global climate modelling: a review. *Atmos. Chem. Phys.* **2005**, *5*, 1053–1123.
- 2) Chung, S. H.; Seinfeld, J. H. Global distribution and climate forcing of carbonaceous aerosols. *J. Geophys. Res.* **2002**, *107*, 4407, doi:10.1029/2001JD001397.
- 3) Tsigaridis, K.; Kanakidou, M. Global modelling of secondary organic aerosol in the troposphere: a sensitivity analysis. *Atmos. Chem. Phys.* **2003**, *3*, 1849–1869.
- 4) Guenther, A.; et al. A global model of natural volatile organic compound emissions. *J. Geophys. Res.* **1995**, *100*, 8873–8892.
- 5) Tuazon, E. C.; Atkinson, R. Product study of the gas-phase reaction of isoprene with the OH radical in the presence of NO_x. *Int. J. Chem. Kinet.* **1990**, *22*, 1221–1236.
- 6) Paulson, S. E.; Flagan, R. C.; Seinfeld, J. H. Atmospheric photooxidation of isoprene, Part I: The hydroxyl radical and ground-state atomic oxygen reactions. *Int. J. Chem. Kinet.* **1992**, *24*, 79–101.

- (7) Miyoshi, A.; Hatakeyama, S.; Washida, N. OH radical-initiated photooxidation of isoprene: An estimate of global CO production. *J. Geophys. Res.* **1994**, *99*, 18,779–18,787.
- (8) Sprengnether, M.; Demerjian, K. L.; Donahue, N. M.; Anderson, J. G. Product analysis of the OH oxidation of isoprene and 1,3-butadiene. *J. Geophys. Res.* **2002**, *107*, D15, 4268, doi: 10.1029/2001JD000716.
- (9) Chen, X.; Hulbert, D.; Shepson, P. B. Measurement of the organic nitrate yield from OH reaction with isoprene. *J. Geophys. Res.* **1998**, *103*, 25,563–25,568.
- (10) Zhao, J.; Zhang, R.; Fortner, E. C.; North, S. W. Quantification of hydroxycarbonyls from OH-isoprene reactions. *J. Am. Chem. Soc.* **2004**, *126*, 2686–2687.
- (11) Baker, J.; Arey, J.; Atkinson, R. Formation and reaction of hydroxycarbonyls from the reaction of OH radicals with 1,3-butadiene and isoprene. *Environ. Sci. Technol.* **2005**, *39*, 4091–4099.
- (12) Pandis, S. N.; Paulson, S. E.; Seinfeld, J. H.; Flagan, R. C. Aerosol formation in the photooxidation of isoprene and β -pinene. *Atmos. Environ.* **1991**, *25A*, 997–1008.
- (13) Edney, E. O.; Kleindienst, T. E.; Jaoui, M.; Lewandowski, M.; Offenber, J. H.; Wang, W.; Claeys, M. Formation of 2-methyl tetrols and 2-methylglyceric acid in secondary organic aerosol from laboratory irradiated isoprene/NO_x/SO₂/air mixtures and their detection in ambient PM_{2.5} samples collected in the eastern United States. *Atmos. Environ.* **2005**, *39*, 5281–5289.
- (14) Claeys, M.; et al. Formation of secondary organic aerosol through photooxidation of isoprene. *Science* **2004**, *303*, 1173–1176.
- (15) Ion, A. C.; Vermeylen, R.; Kourtev, I.; Cafmeyer, J.; Chi, X.; Gelencsér, A.; Maenhaut, W.; Claeys, M. Polar organic compounds in rural PM_{2.5} aerosols from K-pusztá, Hungary, during a 2003 summer field campaign: sources and diel variations. *Atmos. Chem. Phys.* **2005**, *5*, 1805–1814.
- (16) Kourtev, I.; Ruuskanen, T.; Maenhaut, W.; Kulmala, M.; Claeys, M. Observation of 2-methyltetrols and related photo-oxidation products of isoprene in boreal forest aerosols from Hyytiälä, Finland. *Atmos. Chem. Phys.* **2005**, *5*, 2761–2770.
- (17) Claeys, M.; Wang, W.; Ion, A. C.; Kourtev, I.; Gelencsér, A.; Maenhaut, W. Formation of secondary organic aerosols from isoprene and gas-phase oxidation products through reaction with hydrogen peroxide. *Atmos. Environ.* **2004**, *38*, 4093–4098.
- (18) Limbeck, A.; Kulmala, M.; Puxbaum, H. Secondary organic aerosol formation in the atmosphere via heterogeneous reaction of gaseous isoprene on acidic particles. *Geophys. Res. Lett.* **2003**, *30*, 1996–1999.
- (19) Czoschke, N. M.; Jang, M.; Kamens, R. M. Effect of acidic seed on biogenic secondary organic aerosol growth. *Atmos. Environ.* **2003**, *37*, 4287–4299.
- (20) Matsunaga, S.; Mochida, M.; Kawamura, K. Growth of organic aerosols by biogenic semi-volatile carbonyls in the forestal atmosphere. *Atmos. Environ.* **2003**, *37*, 2045–2050.
- (21) Matsunaga, S.; Mochida, M.; Kawamura, K. Variation on the atmospheric concentrations of biogenic compounds and their removal processes in the northern forest at Moshiri, Hokkaido Island in Japan. *J. Geophys. Res.* **2004**, *109*, D04302, doi: 10.1029/2003JD004100.
- (22) Ervens, B.; Feingold, G.; Frost, G. J.; Kreidenweis, S. M. A modeling study of aqueous production of dicarboxylic acids: 1. Chemical pathways and speciated organic mass production. *J. Geophys. Res.* **2003**, *109*, D15205, doi: 10.1029/2003JD004387.
- (23) Lim, H.-J.; Carlton, A. G.; Turpin, B. J. Isoprene forms secondary organic aerosol through cloud processing: model simulations. *Environ. Sci. Technol.* **2005**, *39*, 4441–4446.
- (24) Kroll, J. H.; Ng, N. L.; Murphy, S. M.; Flagan, R. C.; Seinfeld, J. H. Secondary organic aerosol formation from isoprene photo-oxidation under high-NO_x conditions. *Geophys. Res. Lett.* **2005**, *32*, L18808, doi: 10.1029/2005GL023637.
- (25) Cocker, D. R., III; Flagan, R. C.; Seinfeld, J. H. State-of-the-art chamber facility for studying atmospheric aerosol chemistry. *Environ. Sci. Technol.* **2001**, *35*, 2594–2601.
- (26) Keywood, M. D.; Varutbangkul, V.; Bahreini, R.; Flagan, R. C.; Seinfeld, J. H. Secondary organic aerosol formation from the ozonolysis of cycloalkenes and related compounds. *Environ. Sci. Technol.* **2004**, *38*, 4157–4164.
- (27) Drewnick, F.; et al. A new time-of-flight aerosol mass spectrometer (TOF-AMS)—Instrument description and first field deployment. *Aerosol Sci. Technol.* **2005**, *39*, 637–658.
- (28) Atkinson, R.; et al. Evaluated kinetic and photochemical data for atmospheric chemistry: volume 1 – gas-phase reactions of O_x, HO_x, NO_x, and SO_x species. *Atmos. Chem. Phys.* **2004**, *4*, 1461–1738.
- (29) Atkinson, R.; et al. Evaluated kinetic and photochemical data for atmospheric chemistry: Supplement VII, Organic species, *J. Phys. Chem. Ref. Data* **1999**, *28*, 191–393.
- (30) Bahreini, R.; Keywood, M. D.; Ng, N. L.; Varutbangkul, V.; Gao, S.; Flagan, R. C.; Seinfeld, J. H. Measurements of secondary organic aerosol (SOA) from oxidation of cycloalkenes, terpenes, and *m*-xylene using an Aerodyne aerosol mass spectrometer. *Environ. Sci. Technol.* **2005**, *39*, 5674–5688.
- (31) Odum, J. R.; Hoffmann, T.; Bowman, F.; Collins, D.; Flagan, R. C.; Seinfeld, J. H. Gas/particle partitioning and secondary organic aerosol yields. *Environ. Sci. Technol.* **1996**, *30*, 2580–2585.
- (32) Kroll, J. H.; Seinfeld, J. H. Representation of secondary organic aerosol (SOA) laboratory chamber data or the interpretation of mechanisms of particle growth. *Environ. Sci. Technol.* **2005**, *39*, 4159–4165.
- (33) Cocker, D. R., III; Mader, B. T.; Kalberer, M.; Flagan, R. C.; Seinfeld, J. H. The effect of water on gas-particle partitioning of secondary organic aerosol: II. *m*-xylene and 1,3,5-trimethylbenzene photooxidation systems. *Atmos. Environ.* **2001**, *35*, 6073–6085.
- (34) Ng, N. L.; Kroll, J. H.; Keywood, M. D.; Bahreini, R.; Varutbangkul, V.; Flagan, R. C.; Seinfeld, J. H.; Lee, A.; Goldstein, A. H. Contribution of first- versus second-generation products to secondary organic aerosols formed in the oxidation of biogenic hydrocarbons. *Environ. Sci. Technol.* **2006**, in press.
- (35) Tuazon, E. C.; Atkinson, R. A product study of the gas-phase reaction of methyl vinyl ketone with the OH radical in the presence of NO_x. *Int. J. Chem. Kinet.* **1989**, *21*, 1141–1152.
- (36) Tuazon, E. C.; Atkinson, R. A product study of the gas-phase reaction of methacrolein with the OH radical in the presence of NO_x. *Int. J. Chem. Kinet.* **1990**, *22*, 591–602.
- (37) Orlando, J. J.; Tyndall, G. S.; Paulson, S. E. Mechanism of the OH-initiated oxidation of methacrolein. *Geophys. Res. Lett.* **1999**, *26*, 2191–2194.
- (38) Ruppert, L.; Becker, K. H. A product study of the OH radical-initiated oxidation of isoprene: formation of C₅-unsaturated diols. *Atmos. Environ.* **2000**, *34*, 1529–1542.
- (39) Benkelberg, H.-J.; Böge, O.; Seuven, R.; Warneck, P. Product distributions from the OH radical-induced oxidation of but-1-ene, methyl-substituted but-1-enes and isoprene in NO_x-free air. *Phys. Chem. Chem. Phys.* **2000**, *2*, 4029–4039.
- (40) Lee, W.; Baasandorj, M.; Stevens, P. S.; Hites, R. A. Monitoring OH-initiated oxidation kinetics of isoprene and its products using online mass spectrometry. *Environ. Sci. Technol.* **2005**, *39*, 1030–1036.
- (41) Warneke, C.; et al. Isoprene and its oxidation products methyl vinyl ketone, methacrolein, and isoprene related peroxides measured online over the tropical rain forest of Surinam in March 1998. *J. Atmos. Chem.* **2001**, *38*, 167–185.
- (42) McMurry, J. *Organic Chemistry*, 4th ed.; Brooks/Cole: Pacific Grove, CA, 1995.
- (43) Hatakeyama, S.; Izumi, K.; Fukuyama, T.; Akimoto, H.; Washida, N. Reactions of OH with α -pinene and β -pinene in air: estimates of global CO production from the atmospheric oxidation of terpenes. *J. Geophys. Res.* **1991**, *96*, D1, 947–958.
- (44) Zhang, S.-H.; Shaw, M.; Seinfeld, J. H.; Flagan, R. C. Photochemical aerosol formation from α -pinene and β -pinene. *J. Geophys. Res.* **1992**, *92*, D18, 20, 717–720, 729.
- (45) Hurley, M. D.; Sokolov, O.; Wallington, T. J.; Takekawa, H.; Karasawa, M.; Klotz, B.; Barnes, I.; Becker, K. H. Organic aerosol formation during the atmospheric degradation of toluene. *Environ. Sci. Technol.* **2001**, *35*, 1358–1366.
- (46) Johnson, D.; Jenkin, M. E.; Wirtz, K.; Martín-Reviejo, M. Simulating the formation of secondary organic aerosol from the photooxidation of toluene. *Environ. Chem.* **2004**, *1*, 150–165.
- (47) Martín-Reviejo, M.; Wirtz, K. Is benzene a precursor for secondary organic aerosol? *Environ. Sci. Technol.* **2005**, *39*, 1045–1054.
- (48) Song, C.; Na, K.; Cocker, D. R., III Impact of the hydrocarbon to NO_x ratio on secondary organic aerosol formation. *Environ. Sci. Technol.* **2005**, *39*, 3143–3149.
- (49) Presto, A. A.; Huff Hartz, K. E.; Donahue, N. M. Secondary organic aerosol production from ozonolysis: 2. Effect of NO_x concentration. *Environ. Sci. Technol.* **2005**, *39*, 7046.
- (50) Alvarado, A.; Atkinson, R.; Arey, J. Kinetics of the gas-phase reactions of NO₃ radicals and O₃ with 3-methylfuran and the OH radical yield from the O₃ reaction. *Int. J. Chem. Kinet.* **1996**, *28*, 905–909.

- (51) Jenkin, M. E.; Boyd, A. A.; Lesclaux, R. Peroxy radical kinetics resulting from the OH-initiated oxidation of 1,3-butadiene, 2,3-dimethyl-1,3-butadiene and isoprene. *J. Atmos. Chem.* **1998**, *29*, 267–298.
- (52) Docherty, K. S.; Wu, W.; Lim, Y. B.; Ziemann, P. J. Contributions of organic peroxides to secondary organic aerosol formed from reactions of monoterpenes with O₃. *Environ. Sci. Technol.* **2005**, *39*, 4049–4059.
- (53) Bonn, B.; von Kuhlmann, R.; Lawrence, M. G. High contribution of biogenic hydroperoxides to secondary organic aerosol formation. *Geophys. Res. Lett.* **2004**, *31*, L10108, doi: 10.1029/2003GL019172.
- (54) Johnson, D.; Jenkin, M. E.; Wirtz, K.; Martín-Reviejo, M. Simulating the formation of secondary organic aerosol from the photooxidation of aromatic hydrocarbons. *Environ. Chem.* **2005**, *2*, 35–48.
- (55) Tobias, H. J.; Ziemann, P. J. Thermal desorption mass spectrometric analysis of organic aerosol formed from reactions of 1-tetradecene and O₃ in the presence of alcohols and carboxylic acids. *Environ. Sci. Technol.* **2000**, *34*, 2105–2115.
- (56) Lim, Y. B.; Ziemann, P. J. Products and mechanism of secondary organic aerosol formation from reactions of *n*-alkanes with OH radicals in the presence of NO_x. *Environ. Sci. Technol.* **2005**, *39*, 9229–9236.
- (57) Molina, M. J.; Ivanov, A. V.; Trakhtenberg, S.; Molina, L. T. Atmospheric evolution of organic aerosol. *Geophys. Res. Lett.* **2004**, *31*, L22104, doi: 10.1029/2004GL020910.
- (58) Thornton, J. A.; et al. Ozone production rates as a function of NO_x abundances and HO_x production rates in the Nashville urban plume. *J. Geophys. Res.* **2002**, *107*, D12, doi: 10.1029/2001JD000932.
- (59) Presto, A. A.; Huff Hartz, K. E.; Donahue, N. M. Secondary organic aerosol production from terpene ozonolysis. 1. Effect of UV radiation. *Environ. Sci. Technol.* **2005**, *39*, 7036–7045.

Received for review December 3, 2005. Revised manuscript received January 13, 2006. Accepted January 18, 2006.

ES0524301